Journal of Biomedical Optics

SPIEDigitalLibrary.org/jbo

Optical coherence tomography guided microinjections in live mouse embryos: high-resolution targeted manipulation for mouse embryonic research

Saba H. Syed
Andrew J. Coughlin
Monica D. Garcia
Shang Wang
Jennifer L. West
Kirill V. Larin
Irina V. Larina

SPIE

Optical coherence tomography guided microinjections in live mouse embryos: high-resolution targeted manipulation for mouse embryonic research

Saba H. Syed,[a] Andrew J. Coughlin,[b] Monica D. Garcia,[a] Shang Wang,[a] Jennifer L. West,[b] Kirill V. Larin,[a,c] and Irina V. Larina[a,*]
[a]Baylor College of Medicine, Department of Molecular Physiology and Biophysics, One Baylor Plaza, Houston, Texas 77030, United States
[b]Duke University, Department of Biomedical Engineering, Hudson Hall, Durham, North Carolina 27708, United States
[c]University of Houston, Department of Biomedical Engineering, 4605 Cullen Boulevard, Houston, Texas 77204, United States

Abstract. The ability to conduct highly localized delivery of contrast agents, viral vectors, therapeutic or pharmacological agents, and signaling molecules or dyes to live mammalian embryos is greatly desired to enable a variety of studies in the field of developmental biology, such as investigating the molecular regulation of cardiovascular morphogenesis. To meet such a demand, we introduce, for the first time, the concept of employing optical coherence tomography (OCT)-guide microinjections in live mouse embryos, which provides precisely targeted manipulation with spatial resolution at the micrometer scale. The feasibility demonstration is performed with experimental studies on cultured live mouse embryos at E8.5 and E9.5. Additionally, we investigate the OCT-guided microinjection of gold–silica nanoshells to the yolk sac vasculature of live cultured mouse embryos at the stage when the heart just starts to beat, as a potential approach for dynamic assessment of cardiovascular form and function before the onset of blood cell circulation. Also, the capability of OCT to quantitatively monitor and measure injection volume is presented. Our results indicate that OCT-guided microinjection could be a useful tool for mouse embryonic research. [DOI: 10.1117/1.JBO.20.5.051020]

Keywords: optical coherence tomography; mouse embryo; microinjection; real-time imaging; cardiovascular development; gold nanoshells.

Paper 140625SSR received Sep. 29, 2014; accepted for publication Dec. 2, 2014; published online Jan. 12, 2015.

1 Introduction and Background

The capability of injecting cells, contrast agents, dyes, or other agents into specific regions in the mouse embryo is of great importance for biomedical studies of developmental processes.[1–3] Unlike early microinjection approaches[1,4] that are essentially blind procedures with no real-time feedback on the location of needle and the status of the injection, image-guided microinjection has been an attractive approach for conducting targeted delivery in mouse embryos, which brings significant improvement to the molecular and cellular manipulation of embryos at various stages of gestation.[2,3,5] Efforts regarding the development of image-guided microinjection have been mainly focused on employing reflected light microscopy[3,6,7] and ultrasonic imaging techniques[2,5,8–10] for mouse embryos at very early and midgestational stages, respectively. Specifically, Wefers et al. utilize an optical stereomicroscope to monitor the microinjection of mRNA into single-cell mouse embryos for the generation of targeted mouse mutants.[3] The whole injection process can be clearly visualized through the microscope; however, due to a lack of depth resolving capability, this approach has very limited applications for microinjections to the mouse embryos at later gestational stages. High-frequency ultrasonic imaging techniques, such as the ultrasound backscatter microscope,[11] have been used to guide *in utero* microinjections to the mouse embryos from E6.5 to E11.5.[5,9,10] With a spatial resolution that is close to 50 μm, the delivery of cells, contrast agents or virus to the brain,[5,9] the ectoplacental cone,[10] the amniotic cavity,[10] and the anterior limb bud[5] can be real-time monitored with a relatively high precision. Targeting and micromanipulation of the cardiovascular system, the first organ system to fully develop in the embryo, provides a straightforward means to deliver an injectable molecule to embryonic tissue via the vasculature. Furthermore, the early development of the embryonic cardiovascular system is a critical time point in development when embryo viability is highly dependent on cardiovascular form and function. Microinjections to the embryonic cardiovascular system could enable various important applications such as studying the molecular regulation of cardiovascular morphogenesis, or the manipulation and rescue of early embryonic cardiovascular defects. However, such procedures have not been realized (to the best of our knowledge) and could be very challenging with currently available imaging modalities, mainly because the spatial resolution is insufficient to resolve the blood vessels on the embryonic yolk sac. Thus, a depth-resolved imaging technique with better spatial resolution that is suitable for live mouse embryonic imaging is needed for guiding microinjections with small-volume delivery to precise locations within embryonic structures.

Optical coherence tomography (OCT) is a low-coherence three-dimensional (3-D) imaging modality that has the spatial resolution of ~1 to 10 μm with an imaging depth of 1 to 3 mm in most highly scattering tissues,[12–14] which could possibly be used to meet the demand for high-resolution

*Address all correspondence to: Irina V. Larina, E-mail: larina@bcm.edu

0091-3286/2015/$25.00

image-guided microinjection. Besides the major applications in the fields of ophthalmology[15] and cardiology,[16] OCT has been extensively used for embryonic imaging in several animal model systems such as chick,[17–20] quail,[21,22] Xenopus,[23,24] zebrafish,[25,26] mouse,[27–31] and rat.[32] Among these, mouse is an ideal mammalian model for studying the physiological function and pathological process of human organ systems, and various mouse mutants are available to help improve understanding the genetic basis of development and diseases.[33] Applying OCT to mouse embryonic imaging represents an important step for advanced phenotyping of the developmental status.[34–36] Recently, with a primary focus on mouse embryonic cardiovascular development, our group has combined OCT imaging with embryo culturing techniques,[37] and developed methods and protocols for 3-D high-resolution imaging of live mouse embryos during the embryonic days of 7.5 to 10.[28,29,38–40] Specifically, four-dimensional (4-D) OCT imaging of embryonic cardiodynamics has been achieved with nongated data acquisition approaches and computational reconstruction algorithms.[41,42] Also, the employment of Doppler OCT has enabled quantitative hemodynamic analysis in the developing mouse embryo with a spatial resolving ability reaching single moving blood cells.[28,29] Such dynamic imaging capabilities of OCT with both structural and functional information suggest its potential for precise manipulation of mouse embryos.

In this study, we introduce, for the first time, the concept of using OCT for high-resolution image guidance of microinjections in live mouse embryos. We present the procedure and demonstrate the feasibility of OCT-guided microinjections into blood vessels of the yolk sac in the mouse embryos at E8.5 and E9.5. With pilot experiments, we further investigate the possibility of delivering gold–silica nanoshells into the cardiovascular system of mouse embryos under the guidance of OCT, which could be utilized as an approach for studying flow dynamics in the vascular network in response to the initial embryonic heartbeat. We also show the capability of OCT to quantitatively measure injection volume with high sensitivity. Our experimental results indicate that the proposed OCT-guided microinjection in live mouse embryos could be a useful tool for precisely targeted manipulation in mouse embryonic research.

2 Materials and Methods

2.1 *Mouse Embryo Preparation*

Timed matings of CD-1 mice are set overnight and checked for vaginal plugs daily. The day of the observed vaginal plug is counted as E0.5. Embryos are dissected at E8.5 and E9.5 with the yolk sac remaining intact in the culture medium that contains 89% DMEM/F12, 1% Pen-strep solution, and 10% FBS (Life Technologies, Thermo Fisher Scientific Corp.). The dissection station is maintained at 37°C. After dissection, embryos are transferred into a humidified incubator maintained at 37°C, 5% CO_2 and allowed to recover for at least 30 min. The detailed procedure regarding the preparation of mouse embryos can be found in our previous work.[43] To immobilize the embryos during OCT imaging and microinjection, a 2% agarose gel prepared with the culture medium is utilized. Melted gel is poured in a 35-mm diameter culture dish and allowed to solidify with 1 to 2 mm thickness. Prior to transferring the embryo into the culture dish, a small well of about the same size as the embryo is made in the gel and the whole dish is filled with the culture medium. For the OCT-guided microinjection, the embryo within the culture dish is placed in an incubator (humidified, 37°C, 5% CO_2), where the OCT imaging probe and the microinjection setup are located, as shown in Fig. 1.

2.2 *Gold–Silica Nanoshells*

Gold–silica shell-core nanoshells with near-infrared extinction are synthesized via a four-step process as previously described.[44,45] The nanoshells have a diameter of approximately 150 nm with the diameter of the silica core ~120 nm. The sizes of the nanoshells are verified with high contrast-transmission electron microscope imaging, and their optical properties are evaluated using ultraviolet-visible spectroscopy (Varian Cary 50 Bio UV/Visible Spectrophotometer, McKinley Scientific, LLC.). To prevent particle flocculation upon injection in the mouse embryo, the surfaces of the nanoshells are passivated with thiol-terminated poly(ethylene glycol) (PEG-SH, Laysan Bio, MW = 5000 kDa).

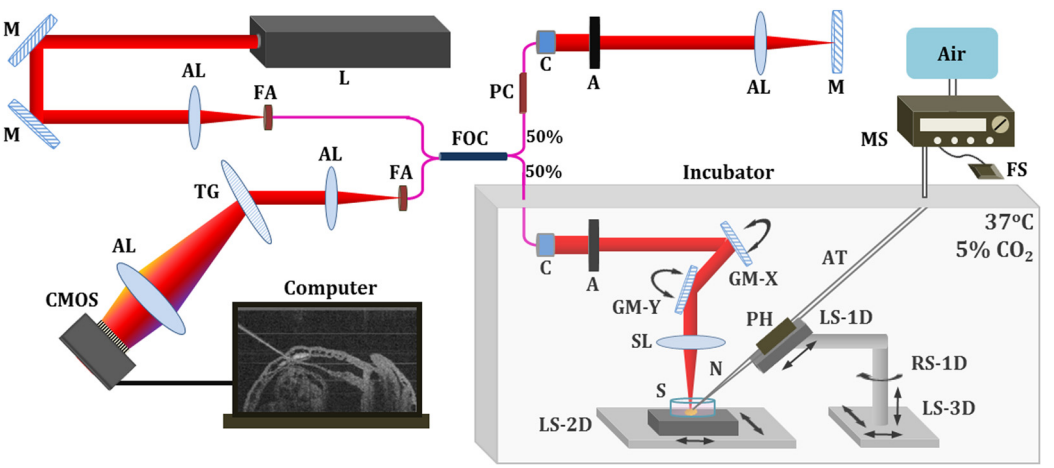

Fig. 1 System setup of OCT-guided microinjection in live mouse embryos. L: laser; M: mirror; AL: achromatic lens; FA: fiber adaptor; TG: transmission gratings; FOC: fiber optic coupler; PC: polarization controller; C: collimator; A: aperture; GM: galvanometer mirror; SL: scan lens; S: sample; MS: microinjection system; FS: foot switch; AT: air tube; PH: pipette holder; N: needle; LS: linear stage; RS: rotational stage.

2.3 *Microinjection Setup*

Quartz capillary pipettes (Sutter Instrument Co.) are pulled on a P-2000 micropipette laser-based puller system (Sutter Instrument Co.). The injection material (3 μl) is loaded into the capillary pipette and the tip of the pipette is then carefully broken using dissecting forceps. The resulted microinjection needle is attached to the pipette holder of the microinjection system (Pico-Injector, Harvard Apparatus Co.) that applies compressed gas for a wide range of delivery volumes of the loaded material. A home-built micromanipulator is used to fix the pipette holder and precisely control the position of the needle with multi-dimensional adjustment (Fig. 1).

2.4 *Spectral Domain Optical Coherence Tomography System and Experimental Methods*

A home-built spectral domain OCT system[46] is utilized for image-guided microinjection. The schematic of the system setup is shown in Fig. 1. The OCT system employs a low-coherence Titanium–Sapphire laser source (Micra-5, Coherence, Inc.) that has a central wavelength of ~808 nm and a bandwidth of ~110 nm. The output of the laser with the collimated beam is coupled into a single-mode fiber and directed to a 50:50 fiber optic coupler. A neutral density filter is utilized to adjust the power that is delivered to the fiber. The light reflected from the reference arm and backscattered from the sample arm forms interference fringes which are detected and spatially resolved by a high-resolution spectrometer with a complementary metal oxide semiconductor line-scanning camera (spL4096-140 k, Basler, Inc.). The OCT system is set to operate at a 50-kHz A-line acquisition speed during the experiments. The axial resolution of the system is measured to be ~5 μm in tissue, and the full width at half maximum of the sample-arm imaging beam at the focal plane is measured to be ~4 μm. Such spatial resolution provides superior resolving capability of the detailed structures inside the mouse embryos. Also, the ~5.5 mm available imaging depth in air enables the capture of most organ and functional systems in the embryos.[43]

For conducting microinjection with the guidance of OCT imaging, the OCT system is operated in the imaging mode of a repeated B-scan that covers a depth-resolved two-dimensional (2-D) field of view (FOV) from the mouse embryo. The position of the injection needle is carefully adjusted to place it within the OCT B-Scan image for real-time continuous visualization of the whole process, including needle insertion and material delivery. As an incubator is utilized to maintain the proper environment for culturing the mouse embryo, during and after the OCT-guided microinjection, the embryo continues its growth. In the pilot experiments for the feasibility studies, saline, fluorescent dextran (Oregon Green®514, 70000 MW, Life Technologies, Thermo Fisher Scientific Corp.), and gold–silica nanoshells have been utilized as the delivery material to the embryonic yolk sac vasculature.

3 Results and Discussions

An example of the OCT-guided microinjection of saline into the extraembryonic vasculature of an E8.5 mouse embryo is presented in Fig. 2. The mouse embryo is dissected, cultured, positioned, and imaged using OCT, where the beating heart and the circulation of blood within both the embryo and the yolk sac vasculature can be clearly observed. The microinjection needle is filled with saline and aligned to appear in the upper left corner

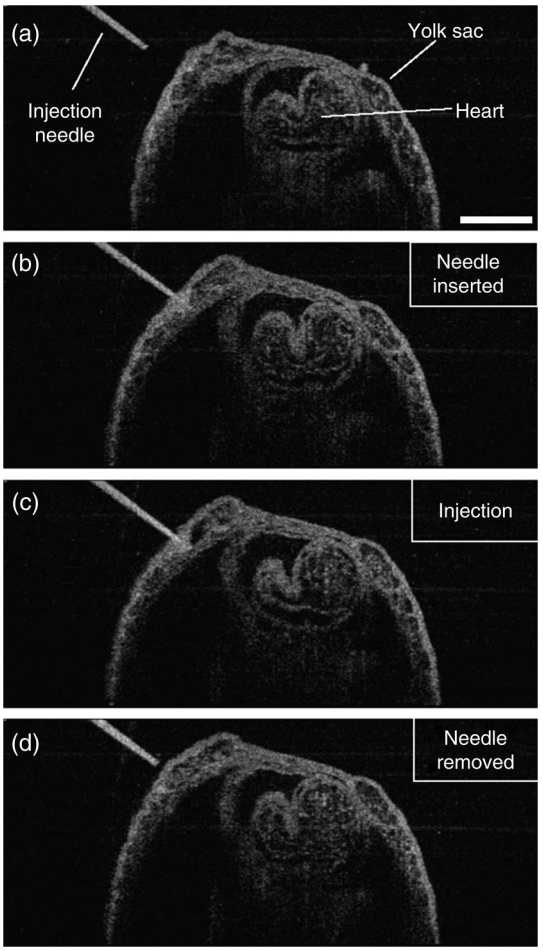

Fig. 2 OCT-guided microinjection of saline in the yolk sac vasculature of a cultured live mouse embryo at E8.5. Real-time continuous optical coherence topography (OCT) B-scan images clearly show the whole microinjection process (Video 1, MOV, 10.1 MB) [URL: http://dx.doi.org/10.1117/1.JBO.20.5.051020.1], including (a) the alignment of the injection needle, (b) the insertion of the needle to a blood vessel of the yolk sac, (c) the injection of saline to the vasculature and (d) the removal of the injection needle. The scale bar corresponds to 300 μm and applies to all figures.

of the OCT B-scan image with the tip close to the blood vessel on the yolk sac, as shown in Fig. 2(a). Upon the alignment of the needle, the real-time OCT imaging is used to guide the insertion of the needle into the yolk sac vasculature without inhibiting the blood circulation, as shown in Fig. 2(b). The injection of saline, which is nonscattering, can be observed from the OCT B-scan image with the dark spot in the targeted vessel and close to the tip of the injection needle, as shown in Fig. 2(c). Monitored by OCT imaging, the removal of the microinjection needle from the yolk sac vasculature reveals no significant leak of blood cells, as shown in Fig. 2(d).

As a further feasibility demonstration of the proposed OCT-guided microinjection, a small volume of fluorescent dextran is injected into the blood circulation of a cultured mouse embryo at E9.5. A 3-D OCT structural image of the embryonic yolk sac is shown in Fig. 3(a), which is characterized by a hierarchical network of large vessels branching out to smaller capillary beds. The dotted line indicates the position of where repeated OCT B-scan images are acquired that are used to guide the microinjection of the florescent dextran into the large vitelline artery.

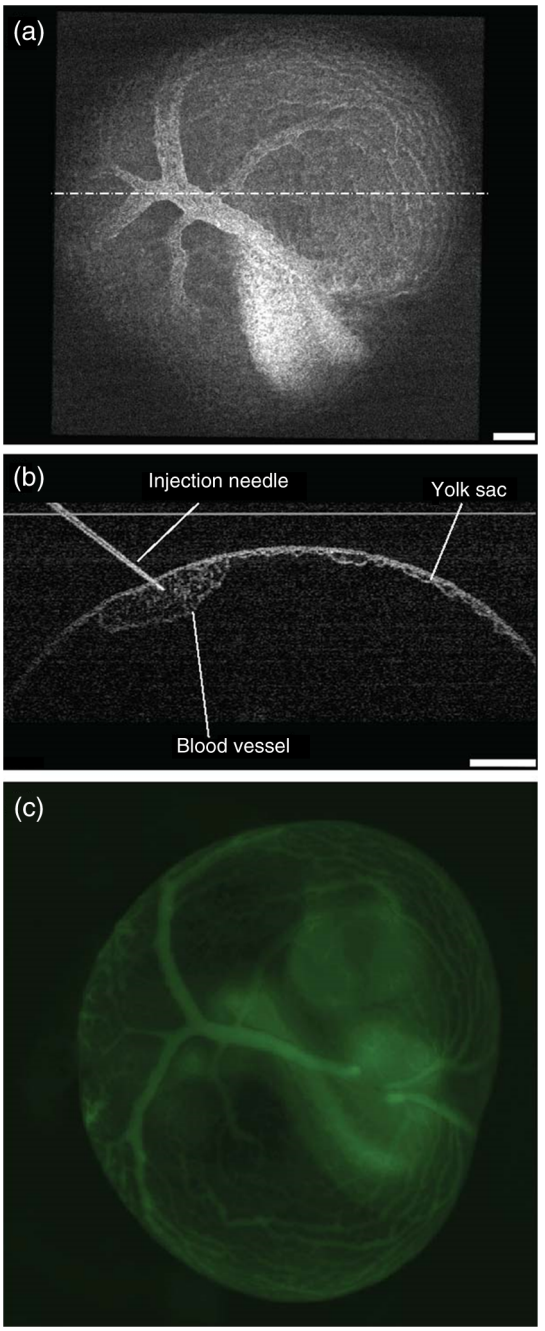

Fig. 3 OCT-guided microinjection of fluorescent dextran mixed with gold–silica nanoshells in the yolk sac vasculature of a cultured live mouse embryo at E9.5 (Video 2, MOV, 8.73 MB) [URL: http://dx.doi.org/10.1117/1.JBO.20.5.051020.2]. (a) Three-dimensional OCT structural image showing the vascular network of the embryonic yolk sac. (b) OCT depth-resolved B-scan image showing the microinjection of fluorescent dextran with the tip of the injection needle inside the targeted vitelline artery. (c) Fluorescent microscopic image of the embryo after microinjection showing fluorescence from dextran labeling the whole vascular network of the embryo, which indicates successful OCT-microinjection with no observable influence on blood flow or heart contraction in the cultured mouse embryo. The scale bars correspond to 300 μm.

Similar procedures, such as the injection of saline, are conducted in this experiment. Based on the 2-D depth-resolved OCT image, the vitelline artery of the yolk sac is precisely targeted. Upon the alignment of the dextran-loaded needle with the OCT B-scan image, the insertion of the needle into the targeted vitelline artery is performed with real-time guidance from OCT, as shown in Fig. 3(b). Once the needle tip is placed at a desired position inside the vessel, injections of fluorescent dextran solution mixed with gold–silica nanoshells are conducted, and then the needle is removed from the yolk sac vasculature. After microinjection, the cultured embryo is immediately imaged using a fluorescent microscope. The resulting fluorescence image presented in Fig. 3(c) shows that the injected fluorescent dextran has filled the whole vasculature network of the yolk sac and the embryo proper due to active circulation, demonstrating successful OCT-guided microinjection. No deleterious influence on blood flow or heart contraction in the cultured mouse embryo has been observed.

Gold–silica nanoshells[44,45] have been identified as a novel contrast agent to enhance OCT imaging. Figure 4(c) shows the normalized extinction spectrum of the nanoshells utilized in this study with a peak position at ~800 nm. For the mouse embryo at early E8.5, the heart has just begun to beat. At this time, only plasma fills the nascent vasculature,

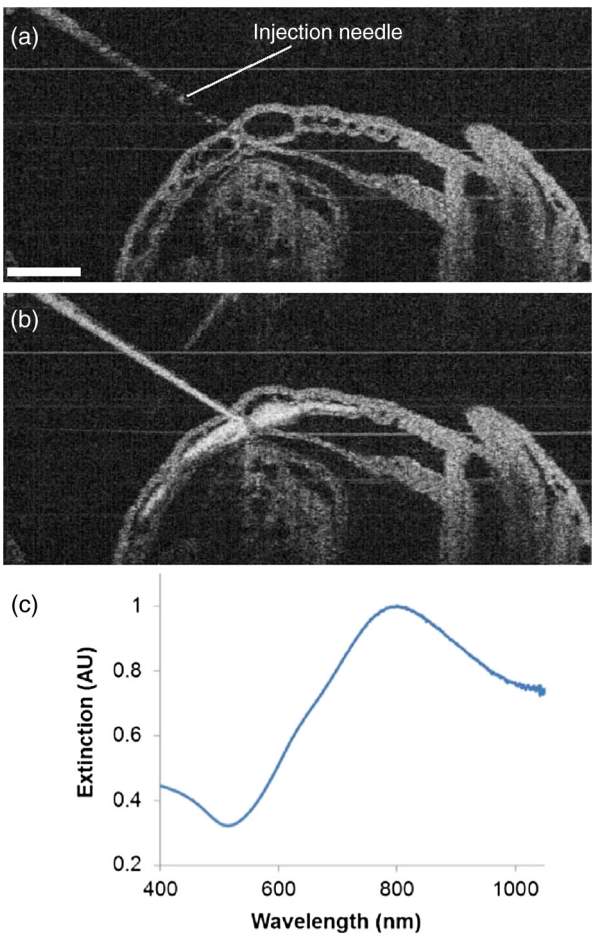

Fig. 4 OCT-guided microinjection of gold–silica nanoshells in the yolk sac vasculature of a cultured live mouse embryo at early E8.5, when the heart just starts to beat. (a) Precise positioning of the injection needle into a vessel of the yolk sac that is only filled with plasma. (b) Microinjection of gold–silica nanoshells into the yolk sac vasculature as a contrast agent for the potential dynamic study of the cardiovascular formation and function before the onset of blood cell circulation. (c) Normalized extinction spectrum of the nanoshells used in this study showing the peak around 800 nm. The scale bar corresponds to 300 μm and also applies for (b).

while red blood cells remain restricted to the blood islands of the yolk sac.[47] Due to the lack of blood cells, the characterization of the flow dynamics in vessels and the assessment of cardiovascular form and function during this gestational stage currently remain very challenging. The delivery of contrast agents to the embryonic vasculature might enable these studies and could potentially be an important application of the proposed OCT-guided microinjections. Such an application is investigated here by performing an injection of gold–silica nanoshells into the blood vessels of the yolk sac of a mouse embryo at this particular developmental stage. Figure 4(a) shows the positioning of the injection needle inside the yolk sac vasculature with the OCT structural image. It can be seen that no OCT signal (scattering of light) is present in the blood vessel, suggesting the absence of red blood cells. Under real-time monitoring with OCT B-scan images, the microinjection of gold–silica nanoshells can be clearly visualized, as shown in Fig. 4(b). Nanoshells provide strong scattering of the light employed by the OCT system, showing significantly increased brightness in the OCT B-scan image, which indicates the potential for the dynamic study of the vasculature and the associated plasma flow in cultured mouse embryos before the introduction of blood cells into the circulation. Our future work will be focused on using functional OCT imaging techniques,[48–50] such as Doppler OCT[28] and speckle variance OCT,[39] to characterize plasma velocity and heart function based on the injected gold–silica nanoshells at this early gestational stage.

The injection volume of material into embryonic structures could be critical to achieve a particular research purpose, and the delivery of an accurate and reproducible microinjection volume is of great importance during microinjections across samples or in longitudinal studies. Due to live feedback, 3-D high-resolution OCT imaging of injected droplets can also be used to guide tuning of the microinjection time and pressure to control the volume of material delivery. Figure 5(a) shows a typical microinjection into mineral oil with an OCT B-scan image. It can be seen that the droplet forming on the tip of the needle appears to have an approximately round shape, which indicates the possibility to conduct a rapid and simple measurement of its volume based on OCT 3-D imaging, as shown in Fig. 5(b). Such an estimation of the volume with OCT is demonstrated to have a sensitivity at the level of nanoliters, as shown in Fig. 5(c), where an increase in volume can be observed with an increase in injection pressure under a constant injection time.

In this paper, the time window for the study and demonstration of OCT-guided microinjection has been focused on the embryonic days of E8.5 and E9.5. These gestational stages correspond to the first 24 h of embryonic cardiodynamics, and are associated with dramatic morphological changes of the heart and the vasculature, and for that reason, are highly important to study in a living system.[51] Thus, we have primarily targeted the vasculature of the yolk sac in cultured live mouse embryos for microinjection in our pilot experiments and investigations. For later stages of gestation (E12.5-E18.5), OCT has been demonstrated with the capability to image various organs, such as the limb, eye, and brain, from live mouse embryos *in utero*.[27,52] Such *in utero* OCT imaging of mouse embryos can be adopted and further developed for OCT-guided *in utero* microinjections while precisely targeting specific organs and detailed structures, which could allow for longitudinal studies after the direct labeling and micromanipulation of particular

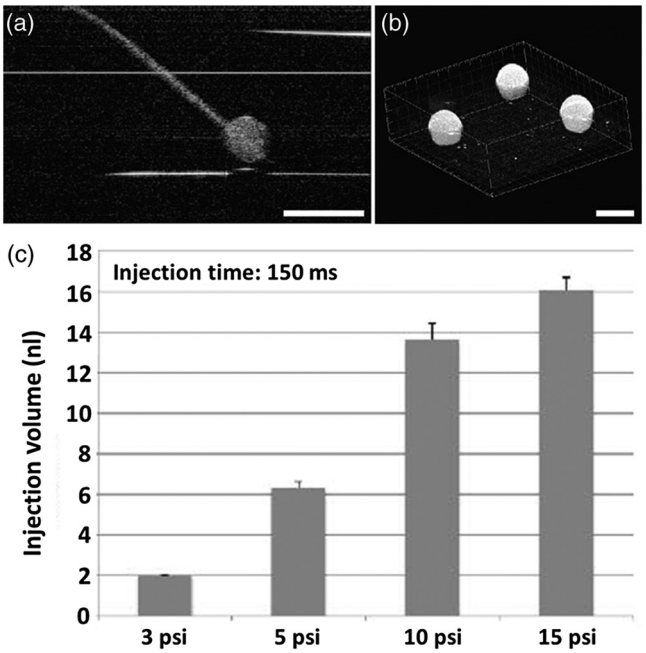

Fig. 5 Three-dimensional (3-D) high-resolution OCT imaging of injected droplets could be used to guide the tuning of microinjection time and pressure. (a) A typical OCT B-scan image of a microinjection into mineral oil showing a droplet forming on the tip of the needle. (b) Three-dimensional OCT imaging of the injected droplets for volume measurement. (c) The volumes of microinjection estimated using OCT at different injection settings, showing an increase in the injected volume associated with an increase in injection pressure, and indicating nano-liter sensitivity of quantitative OCT assessment of the volume of microinjection. The scale bars correspond to 300 μm. In (c), the bars represent the mean values with the standard deviations.

regions in the embryo, which will continue to develop and survive postbirth.

Currently, our proposed OCT-guided microinjections in live mouse embryos rely on repeated OCT B-scan images to provide real-time monitoring of the injection status. A frame rate up to hundreds of Hertz enables sufficient temporal resolving ability for capturing details during the whole microinjection process. However, as only one transverse dimension is available, this limited FOV might result in loss of the needle from OCT depth-resolved images during the injection, and lacks the feasibility to obtain a more thorough visualization of the microinjection process, such as how the injected material spreads over the targeted region. Very recently, Wieser et al. have demonstrated live 4-D OCT imaging with a Fourier domain mode locked laser and advanced GPU processing methods,[53] where a volume rate at tens of Hertz can be achieved. Such ultrafast OCT imaging techniques could possibly improve OCT-guided microinjection with real-time three-dimensional assessment of the targeted injection process in live mouse embryos.

This paper introduces OCT-guided microinjection as a powerful tool for mouse embryonic research, which opens the door for a number of studies of cardiovascular development that require targeted live embryonic manipulation, and potentially enables certain precise micromanipulation approaches that might not be possible with the currently existing image-guided injection techniques. Compared with guided microinjection with ultrasonic imaging,[5,9,10] the proposed method has the major advantage of higher spatial resolution that allows delivery directed into more detailed structures of the mouse embryo, such as the

vascular network. Also, the superior capability of OCT imaging in live mouse embryos[28,29,40] could provide direct characterization of postinjected embryos with both structural and functional information. Such features of OCT-guided microinjection indicate its great potential to complement ultrasound-guided injection and act as an essential approach in mouse embryonic research.

4 Conclusions

A new microinjection approach with guidance from OCT imaging in live mouse embryos is introduced and demonstrated for the first time. We present pilot experiments of OCT-guided microinjections of saline, fluorescent dextran, and gold–silica nanoshells to the yolk sac vasculature of cultured live mouse embryos at E8.5 and E9.5, and investigate the possible application regarding the assessment of cardiovascular form and function before blood cells start to circulate. As a 3-D imaging modality, OCT could also be used to directly characterize microinjection volume, which can help to tune the injection time and pressure for delivering specific volumes of material to targeted regions inside live mouse embryos. The feature of precise manipulation with microscale spatial resolution makes OCT-guided microinjection a useful tool in mouse embryonic research.

Acknowledgments

This work is supported by the National Institutes of Health (R01HL120140 and U54HG006348) as well as by the Optical Imaging and Vital Microscopy core at Baylor College of Medicine.

References

1. R. Jaenisch, "Mammalian neural crest cells participate in normal embryonic development on microinjection into post-implantation mouse embryos," *Nature* **318**(6042), 181–183 (1985).
2. M. Olsson, K. Campbell, and D. H. Turnbull, "Specification of Mouse telencephalic and mid-hindbrain progenitors following heterotopic ultrasound-guided embryonic transplantation," *Neuron* **19**(4), 761–772 (1997).
3. B. Wefers et al., "Generation of targeted mouse mutants by embryo microinjection of TALEN mRNA," *Nat. Protocols* **8**(12), 2355–2379 (2013).
4. R. Jaenisch, "Retroviruses and embryogenesis: microinjection of Moloney leukemia virus into midgestation mouse embryos," *Cell* **19**(1), 181–188 (1980).
5. A. Liu, A. L. Joyner, and D. H. Turnbull, "Alteration of limb and brain patterning in early mouse embryos by ultrasound-guided injection of Shh-expressing cells," *Mech. Dev.* **75**(1–2), 107–115 (1998).
6. B. Wefers et al., "Direct production of mouse disease models by embryo microinjection of TALENs and oligodeoxynucleotides," *Proc. Natl. Acad. Sci.* **110**(10), 3782–3787 (2013).
7. B. Wefers et al., "Generation of targeted mouse mutants by embryo microinjection of TALENs," *Methods* **69**(1), 94–101 (2014).
8. J. C. Slevin et al., "High resolution ultrasound-guided microinjection for interventional studies of early embryonic and placental development in vivo in mice," *BMC Dev. Biol.* **6**(10), (2006).
9. T. J. Pierfelice and N. Gaiano, "Ultrasound-guided microinjection into the mouse forebrain in utero at E9.5," *J. Vis. Exp.* **45**, 1–5 (2010).
10. C. Punzo and C. L. Cepko, "Ultrasound-guided in utero injections allow studies of the development and function of the eye," *Dev. Dyn.* **237**(4), 1034–1042 (2008).
11. D. H. Turnbull et al., "Ultrasound backscatter microscope analysis of early mouse embryonic brain development," *Proc. Natl. Acad. Sci. U. S. A.* **92**(6), 2239–2243 (1995).
12. D. Huang et al., "Optical coherence tomography," *Science* **254**(5035), 1178–1181 (1991).
13. M. E. Brezinski and J. G. Fujimoto, "Optical coherence tomography: high-resolution imaging in nontransparent tissue," *IEEE J. Sel. Topics Quantum Electron.* **5**(4), 1185–1192 (1999).
14. A. M. Zysk et al., "Optical coherence tomography: a review of clinical development from bench to bedside," *J. Biomed. Opt.* **12**(5), 051403 (2007).
15. J. S. Schuman et al., *Optical Coherence Tomography of Ocular Diseases*, SLACK Incorporated, Thorofare, New Jersey (2013).
16. H. G. Bezerra et al., "Intracoronary optical coherence tomography: a comprehensive review: clinical and research applications," *JACC Cardiovasc. Interv.* **2**(11), 1035–1046 (2009).
17. M. Midgett, S. Goenezen, and S. Rugonyi, "Blood flow dynamics reflect degree of outflow tract banding in Hamburger–Hamilton stage 18 chicken embryos," *J. R. Soc. Interface* **11**(100) (2014).
18. T. M. Yelbuz et al., "Optical coherence tomography: a new high-resolution imaging technology to study cardiac development in chick embryos," *Circulation* **106**(22), 2771–2774 (2002).
19. M. W. Jenkins, M. Watanabe, and A. M. Rollins, "Longitudinal imaging of heart development with optical coherence tomography," *IEEE J. Sel. Topics Quantum Electron.* **18**(3), 1166–1175 (2012).
20. P. Li et al., "In vivo functional imaging of blood flow and wall strain rate in outflow tract of embryonic chick heart using ultrafast spectral domain optical coherence tomography," *J. Biomed. Opt.* **17**(9), 096006 (2012).
21. S. Gu et al., "Optical coherence tomography imaging of early quail embryos," *Cold Spring Harb. Protoc.* **2011**(2), pdb.prot5564 (2011).
22. L. M. Peterson et al., "4D shear stress maps of the developing heart using Doppler optical coherence tomography," *Biomed. Opt. Express* **3**(11), 3022–3032 (2012).
23. S. A. Boppart et al., "Noninvasive assessment of the developing Xenopus cardiovascular system using optical coherence tomography," *Proc. Natl. Acad. Sci. U. S. A.* **94**(9), 4256–4261 (1997).
24. V. X. D. Yang et al., "High speed, wide velocity dynamic range Doppler optical coherence tomography (Part II): imaging in vivo cardiac dynamics of Xenopus laevis," *Opt. Express* **11**(14), 1650–1658 (2003).
25. K. Divakar Rao et al., "Noninvasive imaging of ethanol-induced developmental defects in zebrafish embryos using optical coherence tomography," *Birth Defects Res., Part B* **95**(1), 7–11 (2012).
26. L. Kagemann et al., "Repeated, noninvasive, high resolution spectral domain optical coherence tomography imaging of zebrafish embryos," *Mol. Vis.* **14**, 2157–2170 (2008).
27. S. H. Syed et al., "Optical coherence tomography for high-resolution imaging of mouse development in utero," *J. Biomed. Opt.* **16**(4), 046004 (2011).
28. I. V. Larina et al., "Live imaging of blood flow in mammalian embryos using Doppler swept-source optical coherence tomography," *J. Biomed. Opt.* **13**(6), 060506 (2008).
29. I. V. Larina et al., "Hemodynamic measurements from individual blood cells in early mammalian embryos with Doppler swept source OCT," *Opt. Lett.* **34**(7), 986–988 (2009).
30. M. W. Jenkins et al., "Phenotyping transgenic embryonic murine hearts using optical coherence tomography," *Appl. Opt.* **46**(10), 1776–1781 (2007).
31. W. Luo et al., "Three-dimensional optical coherence tomography of the embryonic murine cardiovascular system," *J. Biomed. Opt.* **11**(2), 021014 (2006).
32. I. V. Larina et al., "Live imaging of rat embryos with Doppler swept-source optical coherence tomography," *J. Biomed. Opt.* **14**(5), 050506 (2009).
33. N. Rosenthal and S. Brown, "The mouse ascending: perspectives for human-disease models," *Nat. Cell Biol.* **9**(9), 993–999 (2007).
34. I. V. Larina et al., "Optical coherence tomography for live imaging of mammalian development," *Curr. Opin. Genet. Dev.* **21**(5), 579–584 (2011).
35. I. V. Larina, "Refining imaging strategies to enhance understanding of congenital anomalies," in *SPIE Newsroom* (28 January 2014).
36. I. V. Larina et al., Eds., *Imaging Mouse Embryonic Cardiac Function*, pp. 1035–1043, Cold Spring Harbor Protocols (2012).
37. M. D. Garcia et al., "Live imaging of mouse embryos," *Cold Spring Harb. Protoc.* **2011**(4), pdb.top104 (2011).

38. I. V. Larina et al., "Imaging mouse embryonic cardiovascular development," *Cold Spring Harb. Protoc.* **2012**(10), pdb.top071498 (2012).
39. N. Sudheendran et al., "Speckle variance OCT imaging of the vasculature in live mammalian embryos," *Laser Phys. Lett.* **8**(3), 247–252 (2011).
40. K. V. Larin et al., "Live imaging of early developmental processes in mammalian embryos with optical coherence tomography," *J. Innov. Opt. Health Sci.* **02**(03), 253–259 (2009).
41. I. V. Larina et al., "Sequential turning acquisition and reconstruction (STAR) method for four-dimensional imaging of cyclically moving structures," *Biomed. Opt. Express* **3**(3), 650–660 (2012).
42. S. Bhat et al., "4D reconstruction of the beating embryonic heart from two orthogonal sets of parallel optical coherence tomography slice-sequences," *IEEE Trans. Med. Imaging* **32**(3), 578–588 (2013).
43. M. D. Garcia et al., "Imaging of cardiovascular development in mammalian embryos using optical coherence tomography," *Methods Mol. Biol.* **1214**, 151–161 (2015).
44. A. M. Gobin et al., "Near-infrared resonant nanoshells for combined optical imaging and photothermal cancer therapy," *Nano Lett.* **7**(7), 1929–1934 (2007).
45. A. J. Coughlin et al., "Gadolinium-conjugated gold nanoshells for multimodal diagnostic imaging and photothermal cancer therapy," *Small* **10** (3), 556–565 (2014).
46. S. Wang et al., "Noncontact quantitative biomechanical characterization of cardiac muscle using shear wave imaging optical coherence tomography," *Biomed. Opt. Express* **5**(7), 1980–1992 (2014).
47. K. E. McGrath et al., "Circulation is established in a stepwise pattern in the mammalian embryo," *Blood* **101**(5), 1669–1676 (2003).
48. R. K. Wang et al., "Depth-resolved imaging of capillary networks in retina and choroid using ultrahigh sensitive optical microangiography," *Opt. Lett.* **35**(9), 1467–1469 (2010).
49. E. Jonathan, J. Enfield, and M. J. Leahy, "Correlation mapping method for generating microcirculation morphology from optical coherence tomography (OCT) intensity images," *J. Biophotonics* **4**(9), 583–587 (2011).
50. A. Doronin and I. Meglinski, "Imaging of subcutaneous microcirculation vascular network by double correlation optical coherence tomography," *Laser Photon. Rev.* **7**(5), 797–800 (2013).
51. M. D. Garcia and I. Larina, "Vascular development and hemodynamic force in the mouse yolk sac," *Front. Physiol.* **5** (2014).
52. I. V. Larina et al., "Optical coherence tomography for live phenotypic analysis of embryonic ocular structures in mouse models," *J. Biomed. Opt.* **17**(8), 081410 (2012).
53. W. Wieser et al., "High definition live 3D-OCT in vivo: design and evaluation of a 4D OCT engine with 1 GVoxel/s," *Biomed. Opt. Express* **5**(9), 2963–2977 (2014).

Saba H. Syed received her bachelor's degree in biology from the University of Texas at Arlington in 2007. She completed her master's in biomedical engineering from the University of Houston in 2010. Her research work includes live imaging of mouse embryos in utero and in culture using high resolution optical coherence tomography (OCT).

Andrew J. Coughlin is a senior formulation development chemist at Syngenta. Prior to his current role, he studied the design and application of gold-based nanoparticles for diagnostics and therapeutics in Dr. Jennifer West's Laboratory for Biofunctional Materials at Duke University. He received his PhD degree in bioengineering from Rice University. He has BS degrees in biomedical engineering and textile engineering from North Carolina State University.

Monica D. Garcia is currently a postdoctoral associate at Baylor College of Medicine. She received her BS degree in bioengineering from Rice University in 2004 and her PhD degree in molecular physiology and biophysics from Baylor College of Medicine in 2013. Her research interests include the use of optical coherence tomography for the analysis of cardiogenesis and vascular morphogenesis in mouse embryos.

Shang Wang is currently a postdoctoral associate at Baylor College of Medicine. He received his BS degree in optoelectronic information engineering from Harbin Institute of Technology, China, in 2010 and his PhD degree in biomedical engineering from the University of Houston in 2014. His research interests include the development of noninvasive low-coherence optical techniques for functional imaging of tissue, elastography of ocular and cardiac tissues, and assessment of cilia and embryonic heart dynamics.

Jennifer L. West is a Fitzpatrick Family University professor of engineering in the Department of Biomedical Engineering at Duke University. She received her PhD degree in biomedical engineering from the University of Texas at Austin in 1996. Her research interests include biomaterials, nanotechnology, and tissue engineering.

Kirill V. Larin is an associate professor in the Department of Biomedical Engineering at the University of Houston. He received his PhD degree in biomedical sciences and biomedical engineering from the University of Texas Medical Branch in Galveston in 2002. His research interests include biomedical engineering/optics, with a particular emphasis on diagnostic imaging, biosensing, microscopy, and classification of tissues.

Irina V. Larina is an assistant professor in the Department of Molecular Physiology and Biophysics at Baylor College of Medicine. She received her PhD degree in physiology and biophysics from the University of Texas Medical Branch in Galveston in 2005. Her research interests include the development and application of innovative methods for live dynamic imaging and analysis of mammalian embryonic development.